An extension of 2D Janbu's generalized procedure of slices for 3D slope stability analysis II

—Numerical method and applications

ZHANG Junfeng, LI Zhengguo & QI Tao

Institute of Mechanics, Chinese Academy of Sciences, Beijing 100080, China
Correspondence should be addressed to Zhang Junfeng (email: zhangjf@imech.ac.cn)
Received July 1, 2004

Abstract This paper provides a numerical approach on achieving the limit equilibrium method for 3D slope stability analysis proposed in the theoretical part of the previous paper. Some programming techniques are presented to ensure the maneuverability of the method. Three examples are introduced to illustrate the use of this method. The results are given in detail such as the local factor of safety and local potential sliding direction for a slope. As the method is an extension of 2D Janbu's generalized procedure of slices (GPS), the results obtained by GPS for the longitudinal sections of a slope are also given for comparison with the 3D results. A practical landslide in Yunyang, the Three Gorges, of China, is also analyzed by the present method. Moreover, the proposed method has the advantages and disadvantages of GPS. The problem frequently encountered in calculation process is still about the convergency, especially in analyzing the stability of a cutting corner. Some advice on discretization is given to ensure convergence when the present method is used. However, the problem about convergency still needs to be further explored based on the rigorous theoretical background.

Keywords: slope stability analysis, three-dimensional analysis, limit equilibrium.

DOI: 10.1360/04zze8

1 Introduction

The theoretical formulation for 3D slope stability analysis has been proposed in Part I of this paper. To realize the method in numerical code, some popular software can be used for programming in a transparent manner such as SPREADSHEET-Microsoft Excel and MATHCAD. The geometric shape and characteristics of a slope can also be graphically displayed in the integrated interface of the built-in program.

As the whole calculation procedure for 2D Janbu' method is well known[1,2], the aim will be focused on the calculation of local factor of safety and on the determination of local sliding direction. Comparison is also conducted between the calculated results of

2D and 3D analyses. It should be noted that the results from 2D analysis are for longitudinal sections of a slope while the results from 3D analysis are for the individual blocks or for blocks in the same row/column. Obviously, the longitudinal section is between two adjacent rows/columns. On this point, it is different from the comparison in the existing literatures, such as Chen and Chameau[3], and Zhang[4], in which only one 3D's factor of safety is given.

2 Interpretation on the assumptions in the present method

Lam and Fredlund[5] summarized the knowns and unknowns for solving the three-dimensional factor of safety by the method proposed in their paper. They concluded that the number of assumptions needed to be introduced is $8m\times n$ if a failure mass is divided into m rows and n columns. In the theoretical part of the paper (Part I), the knowns and unknowns in the proposed method are also listed and the assumptions are described.

To further clarify this method, the assumptions introduced should be addressed here: 1) the horizontal shear forces on the sides of the blocks are neglected; 2) the acting point of the thrust force (i.e. thrust line) on the side of the block is a third of the average height of the corresponding side; 3) the normal vector of the bottom surface for each block will be represented by that of a fitting plane, all the acting points of the forces on the bottom surface are at the corresponding geometric center; and 4) the boundary forces are known. The first assumption ensures the thrust forces and shear forces to be solvable and the moment equilibrium around vertical axis to be satisfied naturally. Assumption 1) has been tested numerically in refs. [5, 6]. The second and third assumptions have been widely used in 2D slope stability analysis. Assumption 4) is essential in solving the problem by this method according to the practical boundary.

Moreover, the components of factors of safety $F_x^{i,j}$ for blocks are equal if the blocks are on the same row, and similarly, the components of factors of safety for blocks $F_y^{i,j}$ are equal if the blocks are on the same column. This interpretation is different from conventional definition in most 3D methods in which the whole failure mass is regarded as an integrated one and each block holds the same factor of safety.

3 Programming technique

The programming procedure for this method is the same as for 2D Janbu's method because the third dimension is simultaneously involved in the computing process. The only exception is that 2D analysis gives one value of the factor of safety but this 3D analysis method gives a matrix of factors of safety for all the blocks. The potential sliding direction (expressed by $\beta^{i,j}$, the angle between the direction of the shear force on bottom plane and the x-axis) for each block is determined at the end of the program, while in ref. [7] the directional angle $\beta^{i,j}$ is assumed first and involved in the whole

iterative computing process.

3.1 Discretization

The failure mass is discretized with an $m \times n$ matrix of blocks covering the projection of the whole failure mass on x-y plane. To identify whether there is one of the discretized blocks of the failure mass falling in the $m \times n$ matrix, one can set the element of the matrix to be 1 denoting existence and 0 not. Then every step in the computing process is controlled by the above setting.

As an extension of 2D Janbu's method, this 3D method possesses the advantages and disadvantages of GPS. Some convergence aspects on GPS have been discussed by Chowdhury and Zhang[8]. The following aspect should be given attention in discretization process: the width of the discretized block (i.e. $\Delta x^{i,j}$ and $\Delta y^{i,j}$) should never be too small compared with the height of the block. The presentational reason is that the calculation of the vertical shear force on the lateral side of the block is related to the width of the block and to the selection of the acting point of thrust force. However, the problem about convergency still needs to be further explored based on the rigorous theoretical background.

3.2 Geometric characteristics

The slip surface of each block may be considered as a plane with two dip angles $\alpha_{xz}^{i,j}$ and $\alpha_{yz}^{i,j}$ (Fig. 1). The normal direction of the slip surface is determined by fitting the coordinates of four bottom corners of the block according to the principle of minimum distance. Because the slip surface of a block will never be vertical, the equation of the bottom plane can be assumed as

$$A^{i,j}x + B^{i,j}y + z + D^{i,j} = 0. \tag{1}$$

Then the directional constant of the above equation can be obtained according to the fitting criterion, and the normal vector $n(n_x^{i,j}, n_y^{i,j}, n_z^{i,j})$ of the bottom plane is expressed as

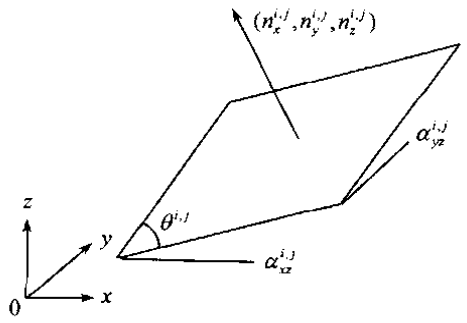

Fig. 1. Fitting bottom plane.

$$n_z^{i,j} = \frac{A^{i,j}}{\sqrt{(A^{i,j})^2 + (B^{i,j})^2 + 1}}, \tag{2}$$

$$n_y^{i,j} = \frac{B^{i,j}}{\sqrt{(A^{i,j})^2 + (B^{i,j})^2 + 1}}, \tag{3}$$

$$n_z^{i,j} = \frac{1}{\sqrt{(A^{i,j})^2 + (B^{i,j})^2 + 1}}. \tag{4}$$

The dip angles $\alpha_{xz}^{i,j}$ and $\alpha_{yz}^{i,j}$ of the bottom plane are also obtained:

$$\alpha_{xz}^{i,j} = \sin^{-1}\left(\frac{A^{i,j}}{\sqrt{1+(A^{i,j})^2}}\right), \tag{5}$$

$$\alpha_{yz}^{i,j} = \sin^{-1}\left(\frac{B^{i,j}}{\sqrt{1+(B^{i,j})^2}}\right). \tag{6}$$

Attention should be given to the above two equations in which the dip angles $\alpha_{xz}^{i,j}$ and $\alpha_{yz}^{i,j}$ are negative when the slope is reversely inclined. The angle $\theta^{i,j}$ between the two components of the shear force $S_{xz}^{i,j}$ and $S_{yz}^{i,j}$ on bottom plane is written as

$$\theta^{i,j} = \cos^{-1}[\sin(\alpha_{xz}^{i,j})\cdot\sin(\alpha_{yz}^{i,j})]. \tag{7}$$

Once the factors of safety $F_x^{i,j}$ and $F_y^{i,j}$ are calculated, the potential sliding direction of the block can be immediately determined according to Part I of this paper:

$$\sin\beta^{i,j} = \frac{F^{i,j}}{F_y^{i,j}}\cdot\sin\theta^{i,j}. \tag{8}$$

One can also express the potential sliding direction by a vector $v(v_x^{i,j}, v_y^{i,j}, v_z^{i,j})$ (also see ref. [7]), it is the reverse direction of the shear force on bottom plane (Fig. 2).

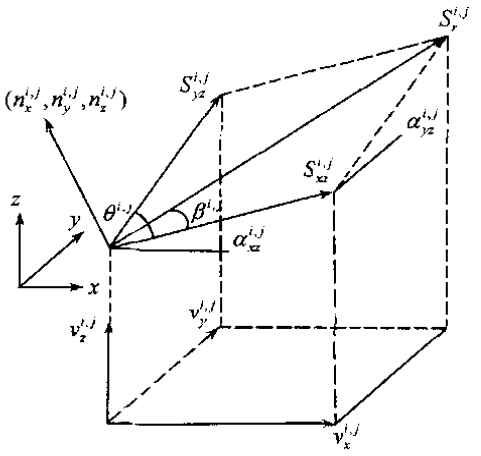

Fig. 2. Geometric characteristics.

$$v_x^{i,j} = \frac{\sin(\theta^{i,j}-\beta^{i,j})\cdot\cos\alpha_{xz}^{i,j}}{\sin\theta^{i,j}}, \tag{9}$$

$$v_y^{i,j} = -\frac{\sin\beta^{i,j}\cdot\cos\alpha_{yz}^{i,j}}{\sin\theta^{i,j}}, \tag{10}$$

$$v_z^{i,j} = -\frac{\sin(\theta^{i,j}-\beta^{i,j})\cdot\sin\alpha_{xz}^{i,j}+\sin\beta^{i,j}\cdot\sin\alpha_{yz}^{i,j}}{\sin\theta^{i,j}}. \tag{11}$$

4 Examples and application of the proposed method

4.1 A symmetrical problem

Example 1 used in Part I of this paper has been referred in refs. [4, 5, 9]. To show how

the proposed method works, the example is still employed here with only simple geological condition being considered. Figs. 3—4 show the geometric feature of the simple slope which the slip surface can be expressed as

$$\frac{x^2}{a^2}+\frac{(y-y_0)}{b^2}+\frac{(z-z_0)^2}{b^2}=1, \tag{12}$$

where y_0 and z_0 are the centric coordinates of the ellipsoid (y_0 = 36.6 m, z_0 = 27.4 m), a and b the half-length of the elliptic revolution's axes in the x, y and z directions (here, a = 46 m and b = 24.4 m).

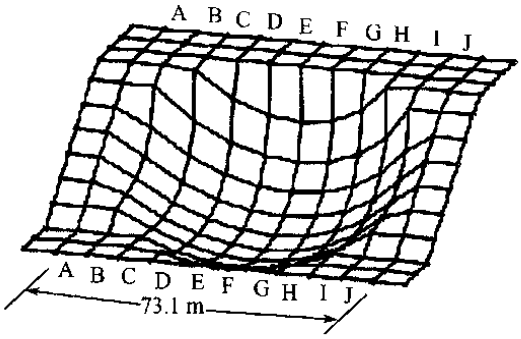

Fig. 3. Concave slip surface of slope 1.

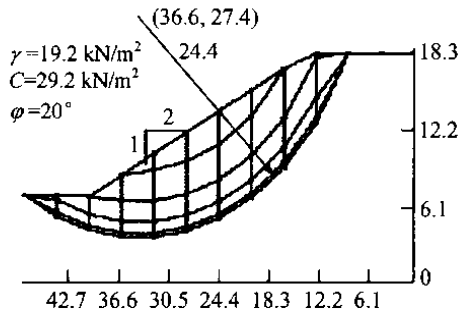

Fig. 4. Longitudinal sections of slope 1.

Because the simple slope is geometric symmetrical about the neutral axis, the factors of safety for the rows in the x-direction are all infinitely large. Then only the factors of safety for the columns calculated by the present method are summarized in table 1 for the simple slope as well as results obtained by 3D simplified Janbu's method. The results using 2D Janbu's method for the longitudinal sections are also presented for comparison. These sections are between two columns represented by A-A, B-B,⋯, and so on (Fig. 3).

The factor of safety for each block can be obtained according to its feature of bottom plane. Since the factor of safety in the x-direction is infinitely large in this symmetrical problem, the final factor of safety for each block is equal to that in the y-direction, as shown in Table 1. Table 2 gives the sliding direction of each block expressed by the angle $\beta^{i,j}$ in eq. (8). Fig. 5 shows the sliding direction of the blocks at a bird view. The projections of the sliding directions for the blocks on the x-y plane are all parallel to the y-axis.

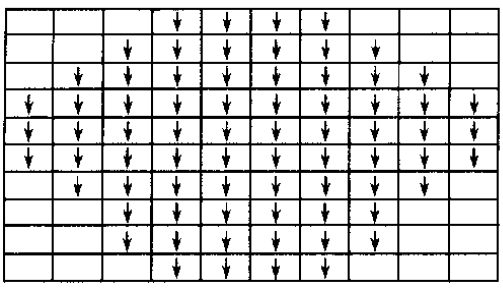

Fig. 5. Sliding direction on x-y plane view.

4.2 Asymmetrical problem 1 —— Half of a concave plane

In this example (different from the example used in the previous paper), the top surface of the slope is still an inclined plane with the dip angle 26.5°. The geometric

Table 1 Comparison of factors of safety calculated by different methods

Method[a)]	Total factor of safety	Factors of safety for each 3D column and 2D section									
		A-A	B-B	C-C	D-D	E-E	F-F	G-G	H-H	I-I	J-J
3DJ	2.126	4.114	2.212	2.046	2.039	2.068	2.068	2.039	2.046	2.212	4.114
3DS	2.096	3.449	2.088	2.006	2.057	2.057	2.057	2.057	2.006	2.088	3.449
2DJ	—	3.279	2.152	1.979	1.941	1.934	1.941	1.979	2.152	3.279	

a) 3DJ, the present 3D method; 3DS, 3D simplified Janbu' method; 2DJ, 2D Janbu's method.

Table 2 The directional angle $\beta^{i,j}$

—	—	—	95.01	91.82	88.18	84.99	—	—	—
—	—	106.0	98.03	92.48	87.52	81.97	74.03	—	—
—	107.5	99.84	95.20	91.641	88.36	84.80	80.16	72.49	—
103.3	100.8	96.33	93.40	91.08	88.92	86.60	83.67	79.21	76.66
100.5	96.18	93.68	91.99	90.63	89.37	88.01	86.32	83.82	79.54
96.35	92.36	91.41	90.77	90.24	89.76	89.23	88.59	87.64	83.65
—	88.78	89.27	89.60	89.87	90.13	90.40	90.73	91.22	—
—	—	87.06	88.41	89.49	90.51	91.59	92.94	—	—
—	—	87.63	87.07	89.07	90.93	92.92	92.37	—	—
—	—	—	88.67	89.37	90.63	91.32	—	—	—

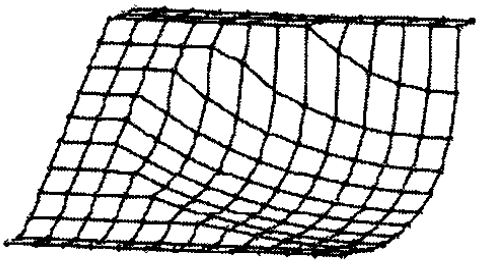

Fig. 6. Ellipsoidal slip surface of slope 2.

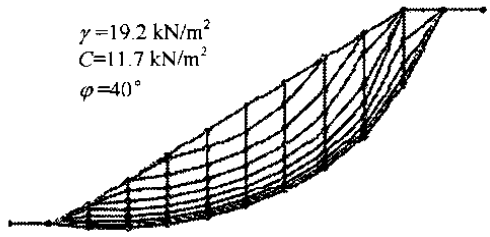

Fig. 7. Longitudinal sections of slope 2.

shape of the failure mass likes a half an ellipsoid, as shown in Figs. 6 and 7. The ellipsoidal slip surface can be expressed as

$$\frac{x^2}{a^2}+\frac{(y-y_0)^2}{b^2}+\frac{(z-z_0)^2}{c^2}=1, \tag{13}$$

in which y_0 = 9.6 m and z_0 = 31.22 m, a, b and c the half-length of the ellipsoidal axes in the x, y and z directions respectively (here, a =65 m, b =55.26 m and c =31.22 m).

The total factor of safety for the simple slope is 2.059. Table 3 gives the factors of safety for the blocks, and Fig. 8 shows the contours of the factors of safety. Table 4 gives the sliding angle $\beta^{i,j}$, and Table 5 transforms $\beta^{i,j}$ to the angle denoting the projection of sliding direction on the x-y plane. Fig. 9 shows the sliding direction of each block at a bird view.

4.3 Asymmetrical problem 2 — a cutting corner

The failure mass in this example is spherical and its top surface is still an inclined

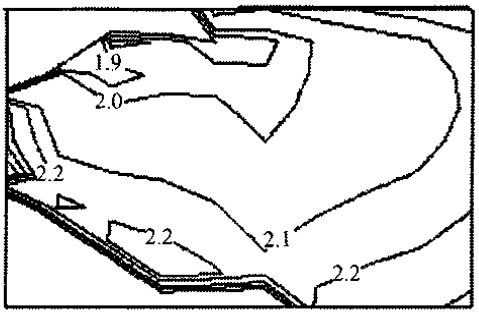

Fig. 8. Contours of factor of safety.

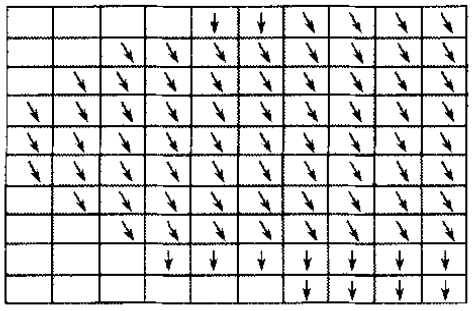

Fig. 9. Sliding direction of the blocks.

Table 3 Factor of safety for each block

—	—	—	—	2.164	2.104	2.178	2.229	2.269	2.324
—	—	1.974	1.942	1.819	1.864	1.960	2.030	2.087	2.170
—	1.965	1.842	1.911	1.925	1.894	1.963	2.014	2.057	2.124
2.352	1.950	1.961	1.976	1.964	1.918	1.977	2.021	2.056	2.116
2.376	2.061	2.035	2.032	2.006	1.949	2.004	2.043	2.074	2.131
2.543	2.150	2.104	2.089	2.054	1.988	2.040	2.077	2.105	2.160
—	2.242	2.179	2.154	2.111	2.035	2.088	2.123	2.150	2.205
—	—	2.251	2.219	2.167	2.083	2.136	2.171	2.197	2.254
—	—	—	2.279	2.227	2.134	2.189	2.224	2.251	2.309
—	—	—	—	—	—	2.241	2.280	2.309	2.372

Table 4 Directional angle $\beta^{i,j}$

—	—	—	—	116.4	110.0	106.4	103.8	101.6	102.7
—	—	129.0	129.2	136.6	125.2	121.0	118.1	115.8	114.1
—	132.2	136.7	128.9	124.5	121.1	119.6	118.4	117.3	116.7
135.4	132.7	127.2	124.1	121.6	119.2	118.6	117.9	117.3	117.1
134.8	126.0	122.8	120.8	119.1	117.2	116.9	116.6	116.3	116.3
128.6	121.2	119.0	117.6	116.3	114.8	114.8	114.6	114.5	114.6
—	116.4	114.7	113.8	112.8	111.5	111.7	111.7	111.6	111.9
—	—	110.0	109.4	108.7	107.7	108.0	108.1	108.2	108.5
—	—	—	104.3	103.2	102.6	103.0	103.2	103.3	103.7
—	—	—	—	—	—	93.86	93.59	93.56	93.71

Table 5 Transforms $\beta^{i,j}$ to the angle by its projection on the x-y plane

—	—	—	—	99.68	103.9	106.7	108.5	109.7	110.3
—	—	119.5	126.1	119.8	118.2	118.3	118.4	118.5	119.1
—	123.0	119.5	119.2	118.5	117.4	118.0	118.4	118.7	119.4
124.6	118.2	117.8	117.7	117.3	116.4	117.1	117.5	117.9	118.5
121.2	116.4	116.1	116.0	115.7	114.9	115.6	116.0	116.4	117.0
119.0	114.3	113.9	113.9	113.6	112.9	113.5	114.0	114.3	114.9
—	111.3	111.1	111.0	110.8	110.1	110.7	111.1	111.4	112.0
—	—	107.7	107.7	107.4	106.9	107.4	107.8	108.0	108.5
—	—	—	103.4	102.9	102.4	102.8	103.1	103.3	103.7
—	—	—	—	—	—	93.56	93.56	93.46	93.68

plane (Fig. 10). Although the failure mass can be considered to be symmetrical about the neural axis, it is discretized by taking the mutually perpendicular side as the x- and

y-axes here in order to show the validity of the method and the correct of the program code. At least, the matrix of the factors of safety must be symmetrical about the converse diagonal corresponding to the neural axis of the slope. But the result for a similar example is not symmetrical in Huang's paper[7] in which the factors of safety F_x and F_y are not equal.

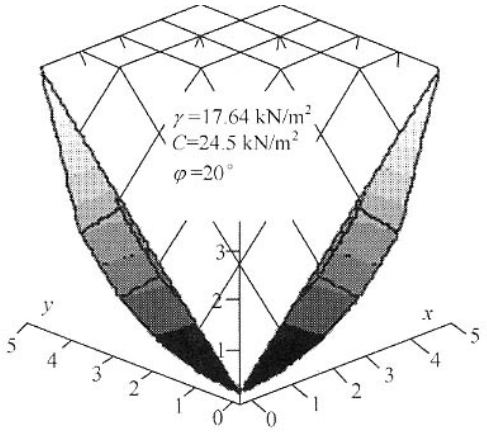

Fig. 10. Geometric feature of the third example.

The failure bottom surface and the top inclined plane of the slope are expressed as

$$\frac{x^2}{a^2}+\frac{y^2}{a^2}+\frac{(z-z_0)^2}{a^2}=1, \tag{14}$$

$$x+y-z=0, \tag{15}$$

where a is the spherical radius, a = 5 m and z_0= 5 m.

The total factor of safety of the slope is 2.614. Table 6 gives the factors of safety and Table 7 gives the sliding directional angle at a bird view. Figs. 11 and 12 are contours of the factors of safety and sliding directions respectively.

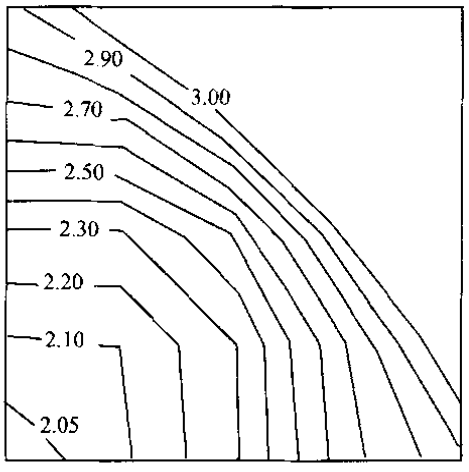

Fig. 11. Contours of factor of safety.

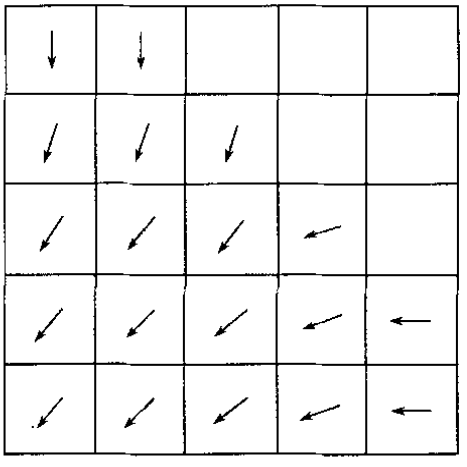

Fig. 12. Sliding direction.

Table 6 Factors of safety for each block

2.869	3.115	—	—	—
2.659	2.688	3.004	—	—
2.287	2.282	2.494	3.004	—
2.077	2.099	2.282	2.688	3.115
2.018	2.077	2.287	2.659	2.869

Table 7 Transforms $\beta^{i,j}$ to the angle by its projection on the x-y plane

89.95	89.95	—	—	—
66.15	65.32	61.91	—	—
51.11	50.00	45.00	28.09	—
46.12	45.00	40.00	24.68	0.05
45.00	43.88	38.89	23.85	0.05

It is shown that this method can be used to analyze various shaped slopes. It also can be used when water pressure is taken into account, like in Part I of this paper. The performance of the present method in the above examples is well except for some special cases, such as a cutting corner employed in ref. [7] in which the maximum thickness and the length of the slope are the same. In this case, the height of the discretized block is far larger than the width and the calculated result will not converge in the iterative process. This case should always be avoided in using the present method.

4.4 A practical landslide of Zhaiba, the Three Gorges, China

The following example is a practical landslide located at the new building site of Zhaiba in Yunyang County, Chongqing, China. The elevation of the landslide is 290—355 m above sea level. The formation of the topographic feature is due to the retrogressive weather action. The main components of the stacked layers are clay, colluvial gravel, and sandstone. The length and width of the sliding mass are 270 and 85 m respectively with total volume 28×10^4—30×10^4 m^3. The average natural unit weight of the soil-stone material is γ_n =21.4 kN/m^3, and the saturated unit weight is γ_s =22.5 kN/m^3. Fig. 13 shows the geological sketch map of the landslide. Fig. 14 is one of the geological sections of the sliding mass.

The total factor of safety calculated by the present method is 1.056. Table 8 is the factors of safety for blocks. Table 9 is the sliding angle projected on the x-y plane. Fig. 15 shows the contours of factors of safety. Fig. 16 illustrates the sliding direction of the failure mass on a bird view.

Compared with the main sliding direction of the real landslide, the calculated result is basically identical with that from geological survey. The factor of safety obtained by 2D GPS is 1.050. The relative flat of slip surface and small slope angle are the main reasons for the results from 2D and 3D analyses being close.

5 Concluding remarks

The numerical program is achieved for the theoretical formulation in Part I of this paper. It is shown that the proposed method performs very well in calculating the factors of safety and potential sliding directions for every part of a slope.

In the present method, the analysis is conducted for the two perpendicular directions (coordinate directions), thus it is certain to give the factor of safety for every row/column. This makes it possible for the comparison between the results from 2D and

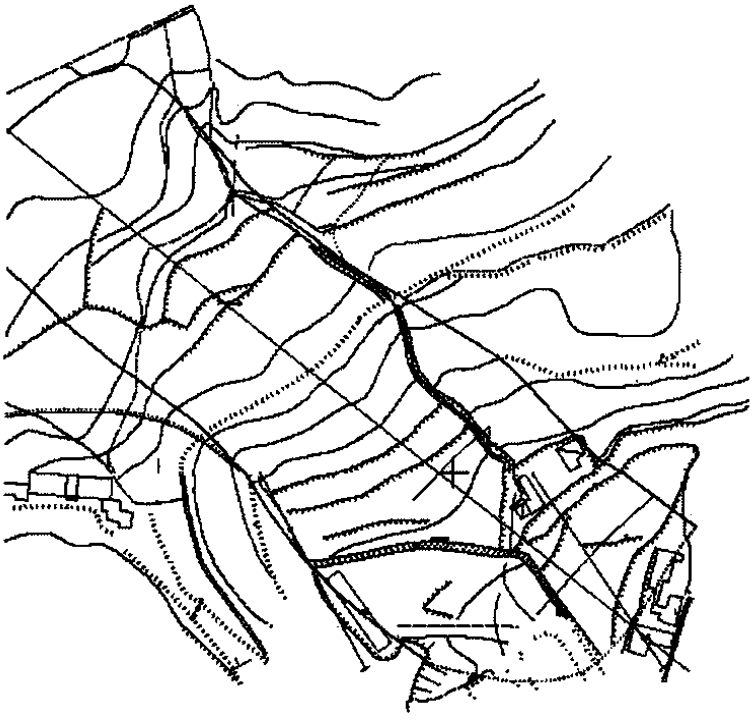

Fig. 13. Zhaiba landslide in Yunyang.

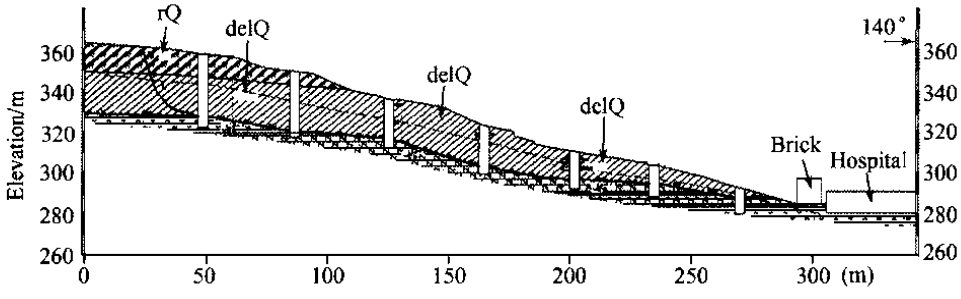

Fig. 14. A cross-section of Zhaiba landslide.

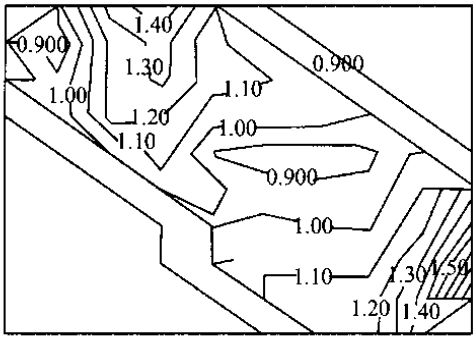

Fig. 15. Contours of factor of safety.

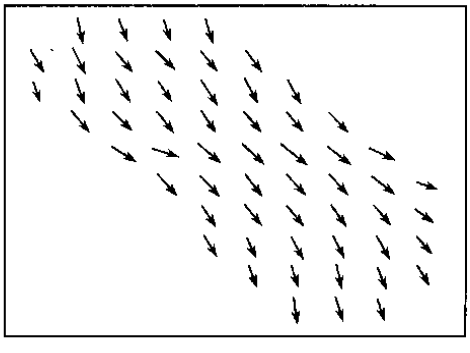

Fig. 16. Calculated sliding direction.

Table 8 Factors of safety for each block

—	0.965	1.335	1.482	1.200	—	—	—	—	—
1.028	0.816	1.217	1.334	1.120	1.048	—	—	—	—
1.109	0.923	1.200	1.326	1.145	1.103	1.074	—	—	—
—	0.916	1.234	1.202	1.045	1.067	1.052	1.011	—	—
—	—	0.994	1.144	0.894	0.857	0.853	0.877	1.029	—
—	—	—	1.053	1.023	0.937	0.912	0.925	1.097	1.360
—	—	—	—	0.990	1.032	0.998	0.989	1.168	1.535
—	—	—	—	1.105	1.069	1.086	1.072	1.302	1.771
—	—	—	—	—	1.141	1.120	1.136	1.423	2.033
—	—	—	—	—	—	1.147	1.147	1.460	—

Table 9 Transforms $\beta^{i,j}$ to the angle by its projection on the x-y plane

—	99.25	104.5	105.0	101.2	—	—	—	—	—
118.9	116.7	130.8	133.4	124.2	120.5	—	—	—	—
108.2	110.3	117.1	121.4	118.9	118.1	116.1	—	—	—
—	124.6	130.8	124.7	122.9	126.7	126.8	124.8	—	—
—	—	144.7	160.3	133.7	133.3	136.5	139.2	150.8	—
—	—	—	130.5	131.1	125.9	126.3	128.6	140.6	158.9
—	—	—	—	120.7	120.8	120.2	120.9	128.2	144.8
—	—	—	—	115.5	112.7	112.0	112.9	118.5	128.8
—	—	—	—	—	105.1	103.7	104.3	107.9	115.3
—	—	—	—	—	—	98.80	98.66	101.0	—

3D analyses for an arbitrary section and its contiguous rows/columns. The comparison is also conducted between this proposed method and 3D simplified Janbu's method. It can be concluded that the proposed method gives larger factor of safety than 2D GPS and 3D simplified Janbu's method, in which the 3D simplified Janbu's method is analyzed by a similar procedure as the proposed method.

As the horizontal inter-block shear force is assumed to be zero, it is inevitable to affect the accuracy for the calculating results, particularly for the sliding direction. Hence, the selection of the coordinate system is very important and it is recommended to set one of the horizontal axes consistent with the practical sliding direction or with potential sliding direction estimated at the beginning of analysis.

Furthermore, the convergence problem should also be explored in theory.

Acknowledgements The authors wish to thank all their colleagues in the Institute of Mechanics, CAS, for their valuable discussion on various parts of the work described in the paper. This work was supported by the National Natural Science Foundation of China (Grant No. 10372104), the Special Funds for the Major State Basic Research Project (Grant No. 2002CB412706), the Knowledge Innovation Project of the Chinese Academy of Sciences (Grant No. KJCX2-SW-L1-2), the Special Research Project for Landslide and Bank-collapse in The Three Gorges Reservoir Areas (Grant No. 4-5).

References

1. Janbu, N., Earth pressure and bearing capacity by generalized procedure of slices, Proceedings of the 4th Int. Conf. of Soil Mechanics, London: Butterworths Scientific Publications, 1957, 2: 207—212.

2. Janbu, N., Slope stability computations, in Embankment-Dam Engineering, New York: John Wiley and Sons, 1973: 47—86.
3. Chen, R. H., Chameau, J. L., Three-dimensional limit equilibrium analysis of slope, Geotechnique, 1982, 32(1): 31—40.
4. Zhang, X., Three-dimensional stability analysis of concave slopes in plane view, J. of Geotechnical Engineering, 1988, 114(6): 658—671.
5. Lam, L., Fredlund, D. G., A general limit equilibrium model for three-dimensional slope analysis, Canadian Geotechnical Journal, 1993, 30: 905—919.
6. Fan, K., Fredlund, D. G., Wilson, G. W., An interslice force function for limit equilibrium slope stability analysis, Canadian Geotechnical Journal, 1986, 23: 287—296.
7. Huang, C. C., Tsai, C. C., New method for 3D and asymmetrical slope stability analysis, J. of Geotechnical and Geoenvironmental Engineering, 2000, 126(10): 917—927.
8. Chowdhury, R. N., Zhang, S., Convergence aspects of limit equilibrium methods for slopes, Canadian Geotechnical Journal, 1990, 27(1): 145—151.
9. Chen, Z., Wang, X., Haberfield, C. et al., A three-dimensional slope stability analysis method using the upper bound theorem, Part I: theory and methods, Int. J. of Rock Mechanics and Mining Sciences, 2001, 38: 369—378.